Metalurgi (2023) 1: 9 - 18

METALURGI
Majalah Ilmu dan Teknologi
p-ISSN 0126-3188 | e-ISSN 2443-3926
ejurnalmaterialmetalurgi.lipi.go.id

SYNTHESIS OF TIN OXIDE NANOCRYSTALLITES WITH VARIOUS CALCINATION TEMPERATURES USING CO-PRECIPITATION METHOD WITH LOCAL TIN CHLORIDE PRECURSOR

Norbert Egan Christo Panthoko[a], Fairuz Septiningrum[a], Akhmad Herman Yuwono[a,*], Eka Nurhidayah[a], Fakhri Akbar Maulana[a], Nofrijon Sofyan[a], Donanta Dhaneswara[a], Tri Arini[b], Lia Andriyah[b], Florentinus Firdiyono[b], Latifa Hanum Lalasari[b], Yahya Winda Ardianto[c], Ria Wardhani Pawan[c]

[a]Department of Metallurgical and Materials Engineering, University of Indonesia
Kampus UI, Kukusan, Depok, Indonesia 16424
[b]Research Center for Metallurgy, National Research and Innovation Agency
B.J. Habibie Sains and Technology Area, Banten, Indonesia 15314
[c]PT Timah Industri
Industrial Estate Cilegon Area (KIEC), Banten, Indonesia 42435
*E-mail: ahyuwono@eng.ui.ac.id

Received: 30-11-2022, Revised: 11-04-2023, Accepted: 12-04-2023

Abstract

Indonesia is one of the largest tin metal producers in the world, and one of its derivative products is tin chloride ($SnCl_4$). This material has been used as a raw ingredient for the production of organotin compounds such as methyltin mercaptide for PVC (polyvinyl chloride) plastic industry as a heat stabilizer. On the other hand, this precursor can be used to synthesize SnO_2 nanomaterials, which have other strategic potentials, including photocatalysts and solar cell applications. In this study, the synthesis of SnO_2 nanocrystallites was carried out using a local tin chloride precursor via the co-precipitation method, followed by a calcination process at temperatures of 300, 400, 500, and 600 °C, for further usage as an ETL (electron transport layer) in a PSC (perovskite solar cell) device. The basic properties characterization was carried out using XRD (X-ray diffraction), ultraviolet-visible (UV-Vis) spectroscopy, and SEM (scanning electron microscopy), while the photocurrent-voltage (I-V) curve photovoltaic performance of the device was performed using a semiconductor parameter analyzer. The characterization results showed that increasing the calcination temperature from 300 to 600 °C increased the average crystallite size from 1.19 to 13.75 nm and decreased the band gap energy from 3.57 to 3.10 eV. The highest PCE (power conversion efficiency) was obtained from the device fabricated with SnO_2 nanocrystallites calcined at a temperature of 300 °C, which was 0.0024%. This result was obtained due to the highest transmittance of this sample as compared to others; the higher the transmittance, the better the performance of the ETL, which in turn increased the overall efficiency of the PSC.

Keywords: *SnO_2 nancrystallites, co-precipitation method, calcination temperature, electron transport layer, perovskite solar cell*

1. INTRODUCTION

Richard Feynman's 1959 scientific speech entitled "There is Plenty Room at the Bottom" paved the way for the rapid development of nanotechnology in today's modern world, from the processes of synthesis and characterization to its applications [1]. An example of its development is the application of metal oxide in gas sensors [2], lithium-ion batteries [3], and solar cells [4]. One of the metal oxides with excellent potential for the development of nanotechnology in Indonesia is SnO_2 (tin oxide). Indonesia has scored in tin production through PT. Timah Tbk, with an increase of 128.7% in 2019 and a total production of 73,390 tons from the previous 33,444 tons in 2018 [5].

DOI : 10.55981/metalurgi.2023.687

Metalurgi is Sinta 2 Journal (https://sinta.kemdikbud.go.id/journals/profile/3708) accredited by Ministry of Education, Culture, Research, and Technology, Republic Indonesia

The use of nanomaterials, especially in the field of renewable energy, has continued to grow until now. It is such a significant opportunity to utilize solar energy sources in Indonesia. With an average daily intensity of solar radiation of 4.8 kWh/m2, Indonesia has the potential to generate more than 207 gigawatts of electrical energy from solar energy sources, beating out hydro, hydrothermal, wind, and ocean waves [6]. The advancement of solar cells, particularly PSC (perovskite solar cells), is needed as an alternative to renewable energy in Indonesia. Concerning this strategic point, SnO_2 could be utilized as an ETL (electron transport layer) material in PSCs.

SnO_2 was chosen as an alternative ETL material due to its excellent electron mobility properties (240 $cm^2/(V.s)$) [7]. In addition, SnO_2 can also be synthesized at low temperatures and produce high efficiency and good PSC stability [8]. Among the various chemical methods for metal oxide nanoparticle preparation, the co-precipitation method has shown good advantages, such as not requiring high temperatures and pressures. Also, filtration and washing can eliminate any impurities left over from the reaction process [9].

In this paper, SnO_2 nanocrystallites were synthesized using local $SnCl_4$ (tin chloride) from PT. Timah Industri by co-precipitation method and calcination at 300, 400, 500, and 600 °C. According to the literature review, no similar research has been conducted on synthesizing SnO2 nanocrystallites for PSC applications from indigenous Indonesian materials. The characterization of the synthesized samples was carried out using XRD (x-ray diffraction), SEM (scanning electron microscope), and UV-Vis spectrophotometer. The PSC device was fabricated and consisted of SnO_2 nanocrystallites as the ETL, with a planar heterojunction architecture of ITO/SnO_2/$CH_3NH_3PbI_3$/Spiro-OMeTAD/Au used for the performance test.

2. MATERIALS AND METHODS

2.1 Materials

The materials used in this study were tin (IV) chloride ($SnCl_4$, PT. Timah Industri), ammonium hydroxide (NH_4OH, Merck), hydrochloric acid (HCl, fuming 37%, Merck), lead (II) iodide (PbI_2, Sigma Aldrich), methylammonium iodide (CH_3NH_3I, Greatcell Solar), dimethylformamide (DMF, Merck), polyethylene glycol (Triton X-100, Sigma Aldrich), Spiro-OMeTAD ($C_{81}H_{68}N_4O_8$, Solaronix), distilled water, acetone, ethanol, and ITO (indium tin oxide) glass substrate. All chemicals in this study were used without further purification.

2.2 Synthesis and Characterization of SnO_2 Nanocrystallites

In water solvent, 0.2 M $SnCl_4$ solution and 0.8 M NH_4OH solution were mixed and stirred until they formed a pH 9 homogenous solution. After that, the precipitate process was carried out for approximately 3 days until a white precipitate was formed, which was then filtered using Whatman filter paper No. 41 and washed with 100 ml of distilled water, and then the precipitate was separated again by the centrifugation method. The white precipitate was washed three times until the pH was close to 7 (neutral). The sample was then dried in an oven at 110 °C for 24 hours to obtain clear crystals of SnO_2, which were then mashed using a mortar to form a powder. Furthermore, the SnO_2 powder was calcined in a muffle furnace for 3 hours at 300, 400, 500, and 600 °C to be further analyzed using XRD (x-ray diffraction), SEM (scanning electron microscope), and UV-Vis spectrophotometer.

The estimation of the average crystallite size of SnO_2 nanocrystallites was calculated according to the following Scherrer's equation [10]:

$$D = \frac{k\lambda}{\beta cos\theta} \quad (1)$$

Where D is the average crystallite size (nm), k is the Scherrer constant (0.9), λ is the wavelength of X-rays, CuKα (1.5406 Å), β is the full width at half maximum/FWHM (radian), and θ is the diffraction angles (degrees).

The optical band gap energy (Eg) of synthesized materials was calculated from absorbance data by using Tauc's equation [11]:

$$(\alpha h\nu)^{1/n} = A(h\nu - E_g) \quad (2)$$

Where α is the absorbance coefficient, hν is the incident photon's energy, A is the proportional constant, and Eg is the optical band gap energy. The exponent value of n indicates the nature of the electron transition in the material, which can be ½ for the direct transition and 2 for the indirect transitions [12].

2.3 Fabrication of Perovskite Solar Cell

Preparation of the ITO glass substrate begins the first stage of PSC fabrication. The 1.5 × 2 cm ITO glass was covered with duct tape, and the rest section was etched with HCl for 15 minutes. Next, the duct tape was removed, and the ITO glass substrate was washed using an ultrasonic

cleaner for 20 minutes with distilled water, acetone, and ethanol, respectively [13].
The second stage is the deposition of the SnO_2 layer onto the ITO glass, prepared in the first stage. SnO_2 slurry was made by mixing the SnO_2 powder with distilled water, acetone, ethanol, and PEG in a ratio of 3:2:4:2:2. This SnO_2 slurry solution was pulverized with a mortar so that it was evenly distributed. The slurry was then deposited onto the ITO glass by the doctor blade method and annealed in the open air at 110 °C for 1 hour [13].
The next stage is the coating of perovskite material ($CH_3NH_3PbI_3$ 0.8 M), obtained by mixing 276 mg PbI2 with 470 mg $CH_3NH_3PbI_3$. The mixed powder was dissolved in 5 mL of DMF and heated at 80 °C for 2 hours. A 100 µL perovskite solution was then dripped onto SnO_2-coated ITO glass and allowed to stand for one minute before spin coating at 3000 rpm for 30 seconds. The SnO_2@perovskite-coated ITO glass was heated at 150 °C for 1 hour in a muffle furnace [13].

Next is the HTL (hole transport layer) coating, which was obtained by dissolving 70 mg of Spiro-OMeTAD in 1 mL of chlorobenzene. After that, the solution was dripped onto SnO_2@perovskite-coated ITO glass and spin-coated for 30 seconds at 3000 rpm. Finally, a thin gold (Au) film was applied to the PSC (perovskite solar cells) configuration using the sputtering method at a pressure of 10-1 mbar and a current of 10 mA for 120 seconds [13]. The structure of the fabricated PSC layer is shown in Fig. 1.

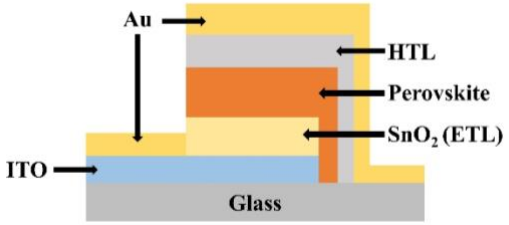

Figure 1. Perovskite solar cell layer structure with planar n-i-p heterojunction configuration

PSC performance testing was conducted to obtain the I-V curve using a semiconductor parameter analyzer (HP Agilent 4145B) with a standard illumination intensity of 100 mW/cm^2. The power conversion efficiency (PCE, η) was then calculated using the equation [14]:

$$\eta = \frac{FF \times I_{sc} \times V_{oc}}{I} \quad (3)$$

Where η is the PCE, is the fill factor, is the short-circuit photocurrent, is the open circuit voltage, and is the illumination intensity used during the test (100 mW/cm^2). While the value of FF was obtained by using the equation [14]:

$$FF = \frac{I_{max} \times V_{max}}{I_{sc} \times V_{oc}} \quad (4)$$

Where and are the current and voltage obtained from the maximum power on the I-V curve, which was obtained from the test results.

3. Result and Discussion

3.1 Crystal Structure Analysis

The formation of SnO_2 nanocrystallites begins with the formation of a white precipitate, $Sn(OH_4)$, in the gel phase, which results from the reaction of $SnCl_4$ with NH_4OH (Eq. (5)). When the white gel is dried, the water vapor is released, leaving behind white SnO_2 crystals (Eq. (6)) [15].

$$SnCl_4 + 4NH_4OH \rightarrow Sn(OH)_4 + 4NH_4Cl \quad (5)$$

$$Sn(OH)_4 \rightarrow SnO_2 + 2H_2O \quad (6)$$

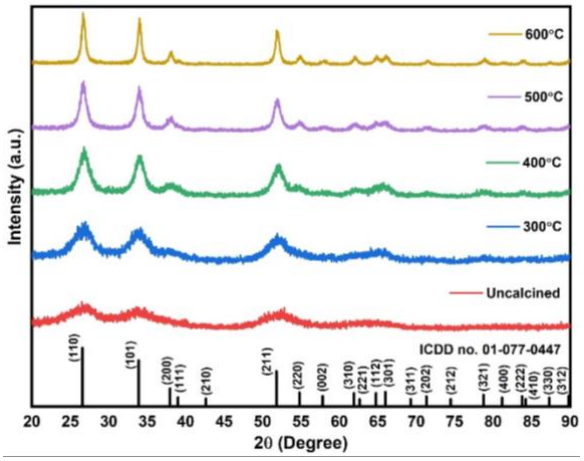

Figure 2. XRD pattern of SnO_2 nanocrystallites samples uncalcined and calcined at 300-600 °C

Figure 2 shows the x-ray diffraction pattern of SnO_2 nanocrystallite samples synthesized by the co-precipitation method with no calcination and with calcination at temperatures ranging from 300 to 600 °C. The diffraction peaks on the graph correspond to the crystal planes (110), (101), and (211) in the ICDD database No. 01-077-0447. This indicates that the synthesized samples had a rutile phase with a tetragonal structure. The graph depicts the sample's crystallinity increases with increasing calcination temperature. This shows that the calcination temperature substantially affect the formation of purified SnO_2 crystals.

According to the XRD graph, SnO_2 nanocrystallite samples that were calcined at temperatures higher than 300 °C have more excellent crystallinity than samples that were calcined at 300 °C or not calcined. When the calcination temperature is increased, the intensity

of the diffraction peak becomes higher and sharper, and the width becomes narrower. This indicates that the precursor obtains sufficient energy to form SnO_2 crystals [15].

The results of calculating the average crystallite size of SnO_2 nanocrystallites with the Scherrer equation (Eq. (1)) are presented in Table 1. The average crystallite size of samples that were not calcined and were calcined at temperatures ranging from 300 to 600 °C has increased from 1.19 to 13.75 nm.

Table 1. The estimation of average crystallite size of SnO_2 nanocrystallites obtained using the Scherrer equation

Calcination temperature (°C)	hkl	2θ (°)	FWHM	The average of crystallite size (nm)
	110	26.42	4.16	
	101	33.94	4.48	
Uncalcined	200	33.94	628.07	1.19
	211	57.68	9.38	
	220	57.90	7.59	
	110	26.76	3.24	
	101	33.84	3.15	
300	200	38.14	3.03	2.04
	211	52.12	3.93	
	220	55.73	617.68	
	110	26.79	1.68	
	101	34.03	1.49	
400	200	45.17	63.22	3.77
	211	52.04	1.82	
	220	65.36	2.76	
	110	26.69	1.17	
	101	33.97	1.04	
500	200	38.04	1.02	6.32
	211	51.92	1.06	
	220	54.56	130.15	
	110	26.72	0.69	
	101	34.01	0.64	
600	200	38.08	0.58	13.75
	211	51.95	0.66	
	220	54.89	0.55	

3.2 Optical Properties Analysis

Figure 3(a) depicts the optical absorbance spectrum of SnO_2 nanocrystallites samples. The curve shows a high absorbance in the ultraviolet region and a low absorbance in the visible light region. The absorbance peak of the sample shifted to the visible light region, or redshifted, as the calcination temperature increased from 300 to 500 °C. This phenomenon affects the optical band gap energy (E_g) of the SnO_2 nanocrystallites samples.

According to the calculation results of the Tauc method (Eq. (2)) in Table 2, the optical band gap energy tends to decrease with increasing calcination temperature, from 3.57 eV (uncalcined) to 2.81 eV (calcined at 500 °C). However, the optical band gap energy was discovered to rise 3.10 eV in the 600 °C calcined sample.

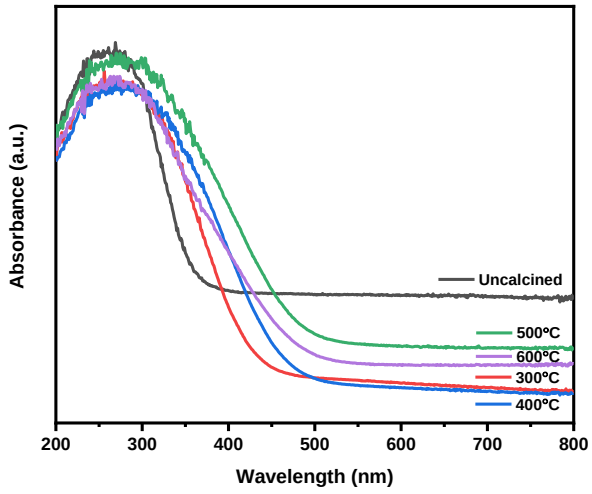

(a)

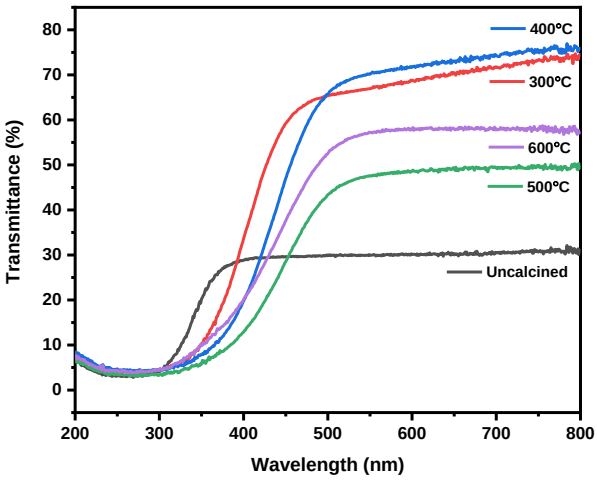

(b)

Figure 3. (a) Absorbance, and (b) transmittance spectra of SnO_2 nanocrystallites samples uncalcined and calcined at 300-600 °C

This conforms to the absorbance spectrum curve of the sample, which also underwent a blueshift.

Table 2. The optical band gap energy (E_g) with increasing calcination temperature

Calcination temperature (°C)	Band gap energy (eV)
Uncalcined	3.57
300	3.18
400	2.95
500	2.89
600	3.10

The size of the crystallite affects the optical band gap energy in a nanoparticle. Due to quantum

effects, the band gap energy of the nanoparticle will decrease with increasing crystallite size and vice versa [16]. In general, the decrease in band gap energy in the SnO_2 samples was consistent with the XRD analysis results, which demonstrated that the average crystallite size grows as the calcination temperature rises.

In the case of the 600 °C calcined sample, the band gap energy has increased again. Meanwhile, the crystallite size has increased due to the received heat energy driving force. There is a possibility that other phases may emerge in minor quantities, which are undetectable by XRD testing but perform an important role in influencing the mechanism of electron excitation from the valence band to the conduction band of SnO_2 nanocrystallites in this study. These nanocrystallites were discovered by UV-Vis spectroscopy at the absorption edge and represented by the optical band gap energy measurement results. However, additional characterization with more advanced tools, such as XANES and XPS, is required to confirm this.
Another explanation that can be related is the influence of the calcination temperature, which has a part in controlling the intrinsic defect in the SnO_2 crystal [17]. The higher the calcination temperature, the more significant the defect reduction, particularly oxygen vacancy, which increases the optical band gap energy [18]. This also happened in a study by Kamble et al., [19], which confirmed an increase in optical band gap energy due to defect reduction of SnO_2 nanocrystallites after the calcination process at 800 °C for 2 hours.

As ETL (electron transport layer) materials, SnO_2 nanocrystallite samples must have high transmittance. So that photons can easily pass through the ETL to the perovskite layer, where electron charge excitation occurs. The overall performance of the PSC (perovskite solar cells) improves with increasing transmittance of the ETL material [20]. For further analysis, the absorbance spectrum of the SnO_2 nanocrystallite samples was processed to obtain the percentage of transmittance using the Lambert-Beer equation as follows [21].

$$T(\%) = 10^{(2-A)} \quad (7)$$

Where T is the percentage of transmittance (%) and A is the absorbance.

As shown in Figure 3(b), the above calculation results were then plotted as a curve between the transmittance percentage and wavelength. According to the transmittance curve, it can be seen that the percentage of transmittance of all SnO_2 nanocrystallites samples increased in the visible light area. Higher transmittance intensities were discovered in SnO_2 nanocrystallite samples that were calcined at 300 and 400 °C. However, the curve for the 300 °C calcined sample has a greater range of light transmittance areas than the curve for the 400 °C calcined sample. This indicates that more photons of light are transmitted to the ETL layer and excite electrons in the perovskite layer in that sample. Therefore, the ETL transmittance performance of the 300 °C calcined sample is greater than that of other samples.

3.3 Surface Morphology Analysis

The surface morphology of the synthesized samples is observable in Fig. 4. According to the SEM observations, the samples tend to aggregate. due to the use of mortar in refining clear SnO_2 crystals into fine SnO_2 powder, which has a very high surface energy that leads to the formation of agglomerates. This result can also be correlated to forming strong hydrogen bonds in the precipitate during the synthesis process [22].

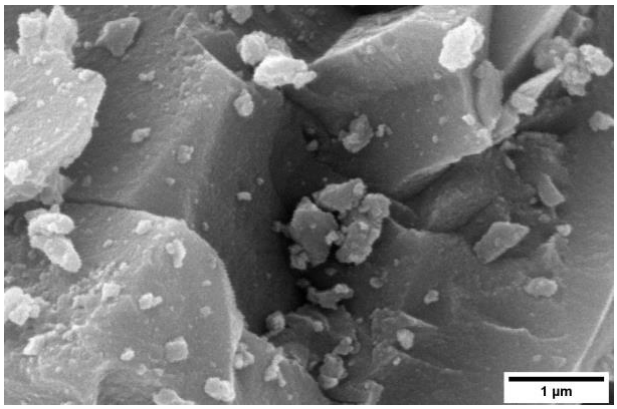

(a)

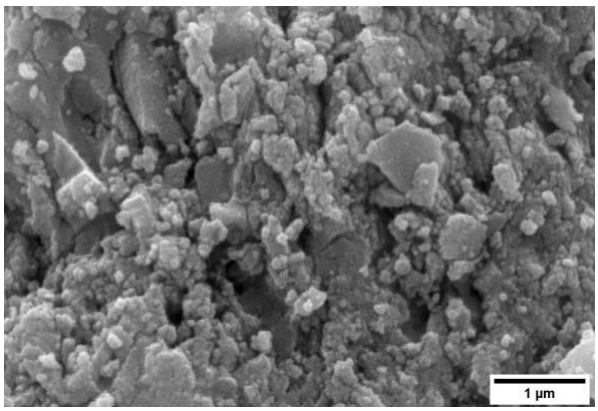

(b)

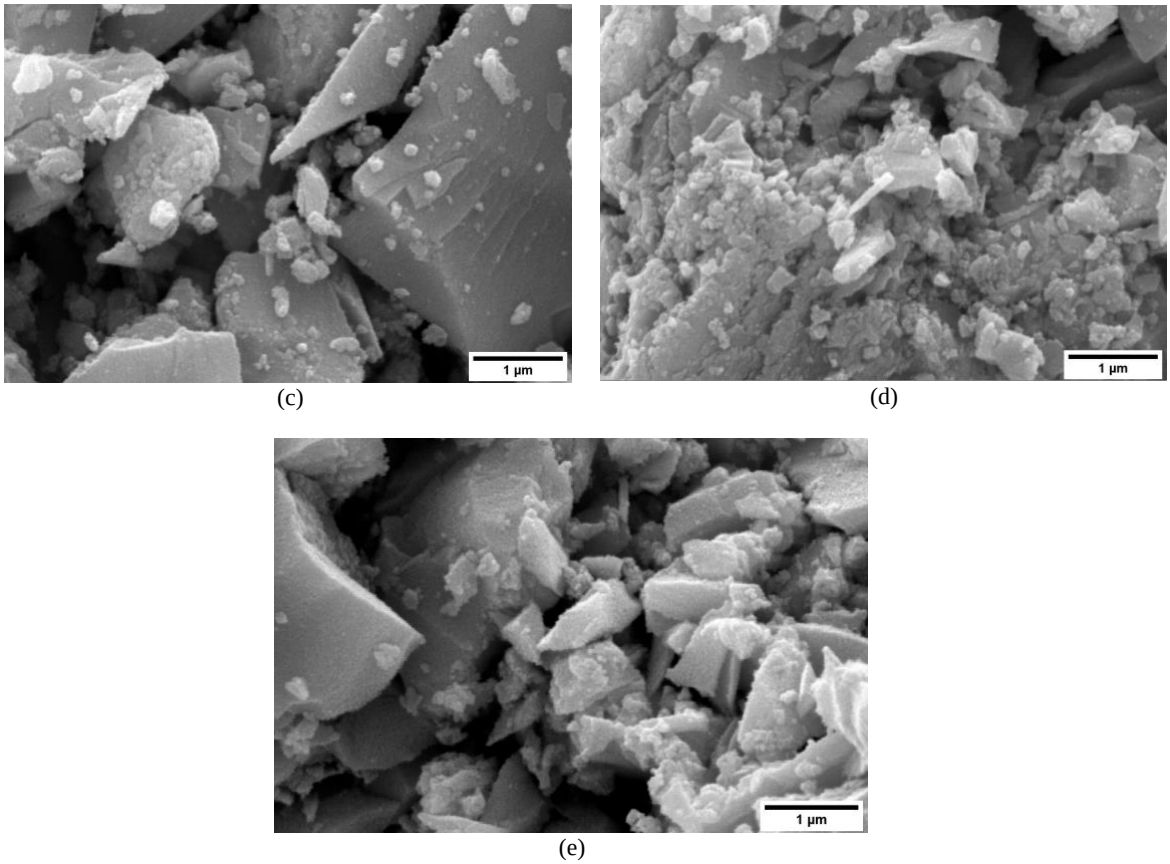

(c) (d)

(e)

Figure 4. Surface morphology of SnO_2 nanocrystallites samples (a) uncalcined and calcined at (b) 300, (c) 400, (d) 500, and (e) 600 °C

3.4 Perovskite Solar Cell Performance

The PSC configuration in this study consisted of ITO/SnO_2/$CH_3NH_3PbI_3$/Spiro-OMeTAD/Au. From the results of processing the I-V curve (Fig. 5), it was determined that only the SnO_2 nanocrystallites sample calcined at 300 °C could serve as an ETL layer and produced the highest PCE (power conversion efficiency), which was 0.0024% (Table 3). In this study, uncalcined and calcined SnO_2 nanocrystallite samples at temperatures other than 300 °C produced no difference in the I-V curve and thus did not affect the PCE.

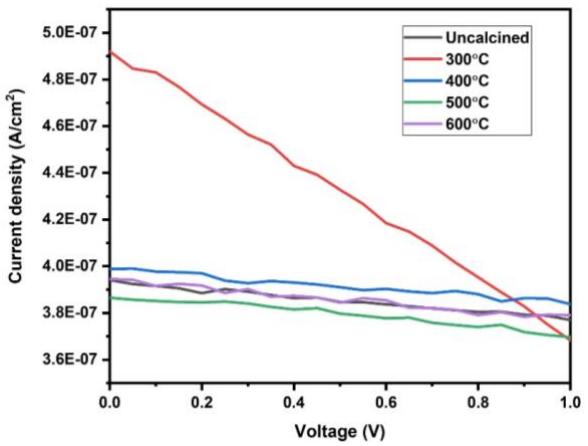

Figure 5. PSC I-V curve with ITO/SnO_2/$CH_3NH_3PbI_3$/Spiro-OMeTAD/Au configuraton

For comparison, in 2016, Jiang et al., [7] used a commercial tin precursor (Alfa Aesar) to produce SnO_2 nanoparticles as ETL through a low-temperature solution process. They achieved a high PCE of almost 20%. The work by Liu et al., [23] uses the same tin precursor and achieves high PCE of 19.38%.

The PSC device fabrication process using SnO_2 nanocrystallite samples, apart from the 300 °C calcined sample, had problems with uneven depositions of the SnO_2 layer onto the ITO glass using the doctor blade method. In addition, the perovskite layer fabrication process carried out in the open air and not in an inert environment also contributed to the low PCE obtained. It has been reported in other studies that most high-efficiency PSC devices are obtained by manufacturing a perovskite layer under inert conditions using a glove box [24].

It is recommended to preserve the substrate at an increased temperature for future fabrication of perovskite solar cell layers using doctor blade deposition in order to obtain a pinhole-free, uniform, and smooth coating. This will increase the solvent evaporation rate, promoting nucleation, and crystal growth [25].

4. CONCLUSION

SnO_2 nanocrystallites have been successfully synthesized using a local tin chloride precursor through the co-precipitation method and calcination treatment at various temperatures of 300, 400, 500, and 600 °C. The crystal structure characterization revealed that the higher the calcination temperature, the higher the crystallinity and the larger the average size of the formed SnO_2 nanocrystallites. The increasing size of crystallites also causes a reduction in band gap energy due to quantum effects. Thus, the calcination treatment in the co-precipitation method affects the characteristics of the resulting SnO_2 nanocrystallites. The SnO_2 nanocrystallites have been applied as an ETL material in PSC with a planar n-i-p heterojunction configuration composed of ITO/SnO_2/$CH_3NH_3PbI_3$/Spiro-OMeTAD/Au.

The highest PSC efficiency was achieved by PSC composed of SnO_2 nanocrystalline with a calcination temperature of 300 °C, which was 0.0024%. This result is following the transmittance level of the sample, which has a wider range of transmittance areas compared to other samples so that more photon energy can pass through the ETL and ultimately improve the overall PSC performance. In this study, the PSC efficiency is still very low. This is because of limitations during making the device, such as the thickness of the layers of the different structures that make up the solar cells and the non-inert condition in which the device is made.

Table 3. Photovoltaic characteristics of the perovskite solar cells based on different calcination temperature

Calcination temperature (°C)	V_{oc} (V)	I_{sc} (A/cm^2)	V_{maks} (V)	I_{maks} (A/cm^2)	FF	PCE (%)
Uncalcined	5	0.0001	2.7	0.0001	0.2922	0.0001
300	5	0.0013	3.35	0.0007	0.3747	0.0024
400	5	0.0001	2.9	0.0001	0.3975	0.0001
500	5	0.0001	2.7	0.0001	0.3038	0.0001
600	5	0.0001	2.5	0.0001	0.2834	0.0001

ACKNOWLEDGMENT

We gratefully acknowledge Direktorat Riset dan Pengabdian Masyarakat Universitas Indonesia (DRPM-UI) for research funding support through International Indexed Publication Grants (PUTI) 2020 (No. NKB-3702/UN2.RST/HKP.05.00/2020) and PT. Timah Industri for providing tin chloride precursor.

REFERENCES

[1] J. E. Hulla, S. C. Sahu, and A. W. Hayes, "Nanotechnology: History and future," *Hum. Exp. Toxicol.*, vol. 34, no. 12, pp. 1318-1321, 2015. Doi: 10.1177/0960327115603588.

[2] W. Chen, Q. Zhou, F. Wan, and T. Gao, "Gas sensing properties and mechanism of nano-SnO_2-based sensor for hydrogen and carbon monoxide," *J. Nanomater.*, vol. 2012, no. 612420, 2012. Doi: 10.1155/2012/612420.

[3] C. P. Wu, K. X. Xie, J. P. He, Q. P. Wang, J. M. Ma, S. Yang, and Q. H. Wang, "SnO_2 quantum dots modified N-doped carbon as high-performance anode for lithium ion batteries by enhanced pseudocapacitance," *Rare Met.*, vol. 40, no. 1, pp. 48-56, 2021. Doi: 10.1007/s12598-020-01623-x.

[4] H. Min, D. Y. Lee, J. Kim, G. Kim, K. S. Lee, J. Kim, M. J. Paik, Y. K. Kim, K. S. Kim, M. G. Kim, T. J. Shin, and S. I. Seok, "Perovskite solar cells with atomically coherent interlayers on SnO_2 electrodes," *Nature*, vol. 598, no. 7881, pp. 444-450, 2021. Doi:10.1038/s41586-021-03964-8.

[5] PT. Timah Tbk.," Membangun ketahanan dan meraih performa progresif," Laporan Tahunan Annual Report 2021. Available: https://timah.com/userfiles/post/220428626A5287E3839.pdf. [Diakses tanggal: 26 Juli 2022]

[6] Pusat Pengkajian Industri Proses dan Energi (PPIPE)," Outlook energi Indonesia 2021 perspektif teknologi energi Indonesia: Tenaga surya untuk penyediaan energi charging station," Badan Pengkajian dan Penerapan Teknologi (BPPT). Jakarta. Available: https://www.bppt.go.id/dokumen/file/865/download [Diakses tanggal: 26 Juli 2022]

[7] Q. Jiang, L. Zhang, H. Wang, X. Yang, J. Meng, H. Liu, Z. Yin, J. Wu, X. Zhang, and J. You, "Enhanced electron extraction

using SnO_2 for high-efficiency planar-structure $HC(NH_2)_2$ PbI_3-based perovskite solar cells," *Nat. Energy*, vol. 2, no. 1, 2017. Doi:10.1038/nenergy.2016.177.

[8] G. Yang, P. Qin, G. Fang, and G. Li, "Tin oxide (SnO_2) as effective electron selective layer material in hybrid organic-inorganic metal halide perovskite solar cells," *J. Energy Chem.*, vol. 27, no. 4, pp. 962-970, 2018. Doi: 10.1016/j.jechem.2018.03.018.

[9] S. Tazikeh, A. Akbari, A. Talebi, and E. Talebi, "Synthesis and characterization of tin oxide nanoparticles via the co-precipitation method," *Mater. Sci. Pol.*, vol. 32, no. 1, pp. 98-101, 2014. Doi: 10.2478/s13536-013-0164-y.

[10] C. Karunakaran, S. Sakthi Raadha, and P. Gomathisankar, "Microstructures and optical, electrical and photocatalytic properties of sonochemically and hydrothermally synthesized SnO_2 nanoparticles," *J. Alloys Compd.*, vol. 549, pp. 269-275, 2013. Doi: 10.1016/j.jallcom.2012.09.035.

[11] Ł. Haryński, A. Olejnik, K. Grochowska, and K. Siuzdak, "A facile method for Tauc exponent and corresponding electronic transitions determination in semiconductors directly from UV–Vis spectroscopy data," *Opt. Mater. (Amst).*, vol. 127, 2022. Doi: 10.1016/j.optmat.2022.112205.

[12] Y. Wang, L. Tan, and L. Wang, "Hydrothermal synthesis of SnO_2 nanostructures with different morphologies and their optical properties," *J. Nanomater.*, vol. 2011, no. 529874, 2011. Doi: 10.1155/2011/529874.

[13] N. Sofyan, A. Ridhova, Salman, A. H. Yuwono, and A. Udhiarto, "Synthesis and characterization of nano rosette TiO_2 and $CH_3NH_3PbCl_2I$ for potential use in perovskite solar cell," *IOP Conf. Ser. Mater. Sci. Eng.*, vol. 541, no. 1, 2019. Doi:10.1088/1757-899X/541/1/012048.

[14] S. Günes, and N. S. Sariciftci, "Hybrid solar cells," *Inorganica Chim. Acta*, vol. 361, no. 3, pp. 581-588, 2008. Doi: 10.1016/j.ica.2007.06.042.

[15] P. Khaenamkaew, D. Manop, C. Tanghengjaroen, and W. P. N. Ayuthaya, "Crystal structure, lattice strain, morphology, and electrical properties of SnO_2 nanoparticles induced by low calcination temperature," *Adv. Mater. Sci. Eng.*, vol. 2020, no. 3852421, 2020. Doi: 10.1155/2020/3852421.

[16] R. Viter, A. Katoch, and S. S. Kim, "Grain size dependent bandgap shift of SnO_2 nanofibers," *Met. Mater. Int.*, vol. 20, no. 1, pp. 163-167, 2014. Doi: 10.1007/s12540-013-6027-6.

[17] S. Mehraj, M. S. Ansari, and A. A. Al-ghamdi, "Annealing dependent oxygen vacancies in SnO_2 nanoparticles: structural, electrical and their ferromagnetic behavior," *Mater. Chem. Phys.*, vol. 171, pp. 109-118, 2016. Doi: 10.1016/j.matchemphys.2015.12.006.

[18] J. Ungula, B. F. Dejene, and H. C. Swart, "Effect of pH on the structural, optical and morphological properties of Ga-doped ZnO nanoparticles by reflux precipitation method," *Phys. B Condens. Matter*, vol. 535, pp. 251-257, 2018. Doi:10.1016/j.physb.2017.07.052.

[19] V. B. Kamble, and A. M. Umarji, "Defect induced optical bandgap narrowing in undoped SnO_2 nanocrystals," *AIP Adv.*, vol. 3, no. 8, 2013. Doi: 10.1063/1.4819451.

[20] Y. Chen, Q. Meng, L. Zhang, C. Han, H. Gao, Y. Zhang, and H. Yan, "SnO_2-based electron transporting layer materials for perovskite solar cells: A review of recent progress," *J. Energy Chem.*, vol. 35, pp. 144-167, 2019. Doi: 10.1016/j.jechem.2018.11.011.

[21] D. F. Swinehart, "The beer-lambert law," *J. Chem. Educ.*, vol. 39, no. 7, pp. 333, 1962.

[22] J. Divya, A. Pramothkumar, S. J. Gnanamuthu, D. C. B. Victoria, and P. C. J. Prabakar, "Structural, optical, electrical and magnetic properties of Cu and Ni doped SnO_2 nanoparticles prepared via co-precipitation approach," *Phys. B Condens. Matter*, vol. 588, no. 2019, pp. 412169, 2020. Doi: 10.1016/j.physb.2020.412169.

[23] J. Liu, N. Li, Q. Dong, J. Li, C. Qin, and L. Wang, "Tailoring electrical property of the low-temperature processed SnO_2 for high-performance perovskite solar cells," *Sci. China Mater.*, vol. 62, no. 2, pp. 173-180, 2019. Doi:10.1007/s40843-018-9305-6.

[24] M. Lv, X. Dong, X. Fang, B. Lin, S. Zhang, X. Xu, J. Ding, and N. Yuan, "Improved photovoltaic performance in perovskite solar cells based on $CH_3NH_3PbI_3$ films fabricated under

controlled relative humidity," *RSC Adv.*, vol. 5, no. 114, pp. 93957-93963, 2015. Doi:10.1039/c5ra14587b.

[25] D. Wang, J. Zheng, X. Wang, J. Gao, W. Kong, C. Cheng, and B. Xu, "Improvement on the performance of perovskite solar cells by doctor-blade coating under ambient condition with hole-transporting material optimization," *J. Energy Chem.*, vol. 38, pp. 207-213, 2019. Doi:10.1016/j.jechem.2019.03.023.